



PNNL-24160

Prepared for the U.S. Department of Energy
under Contract DE-AC05-76RL01830

The Microstructure of Rolled Plates from Cast Billets of U-10Mo Alloys

EA Nyberg
DE Burkes

VV Joshi
CA Lavender

March 2015



Pacific Northwest
NATIONAL LABORATORY

*Proudly Operated by **Battelle** Since 1965*

DISCLAIMER

This report was prepared as an account of work sponsored by an agency of the United States Government. Neither the United States Government nor any agency thereof, nor Battelle Memorial Institute, nor any of their employees, makes **any warranty, express or implied, or assumes any legal liability or responsibility for the accuracy, completeness, or usefulness of any information, apparatus, product, or process disclosed, or represents that its use would not infringe privately owned rights.** Reference herein to any specific commercial product, process, or service by trade name, trademark, manufacturer, or otherwise does not necessarily constitute or imply its endorsement, recommendation, or favoring by the United States Government or any agency thereof, or Battelle Memorial Institute. The views and opinions of authors expressed herein do not necessarily state or reflect those of the United States Government or any agency thereof.

PACIFIC NORTHWEST NATIONAL LABORATORY
operated by
BATTELLE
for the
UNITED STATES DEPARTMENT OF ENERGY
under Contract DE-AC05-76RL01830

Printed in the United States of America

Available to DOE and DOE contractors from the
Office of Scientific and Technical Information,
P.O. Box 62, Oak Ridge, TN 37831-0062;
ph: (865) 576-8401
fax: (865) 576-5728
email: reports@adonis.osti.gov

Available to the public from the National Technical Information Service
5301 Shawnee Rd., Alexandria, VA 22312
ph: (800) 553-NTIS (6847)
email: orders@ntis.gov <<http://www.ntis.gov/about/form.aspx>>
Online ordering: <http://www.ntis.gov>



This document was printed on recycled paper.

(8/2010)

The Microstructure of Rolled Plates from Cast Billets of U-10Mo Alloys

EA Nyberg
DE Burkes

VV Joshi
CA Lavender

March 2015

Prepared for
the U.S. Department of Energy
under Contract DE-AC05-76RL01830

Pacific Northwest National Laboratory
Richland, Washington 99352

Executive Summary

Thirteen samples of rolled plates from three separate castings of uranium, alloyed with 10 wt% molybdenum (U-10Mo) were sent from the Y-12 National Security Complex (Y12) to the Pacific Northwest National Laboratory (PNNL) for microstructural characterization. These samples were taken from castings that were 25.4 mm (1.0 in.) thick and then hot rolled to nominally 3 mm (0.12 in.) thick. The details of the casting, rolling and cutting processes are described in a series of separate Y-12 technical reports. In this study, the microstructure found in the samples from the plates were highly variable and ranged from uniform equiaxed grains to oxygen-rich inclusions that were through-thickness. Aside from the large oxygen-rich inclusions, typically there were two distinct regions observed in the samples: one region with a Mo-lean and Mo-rich area and a second region containing an inhomogeneous non-stoichiometric oxygen-rich phase. Two samples from one casting also contained large UO_2 -rich inclusions.

Characterization was conducted on eight samples from the Y-12 hot-rolled casting 3K32-A5-VMVE. Two hot-rolled samples from casting 3K32-A6-VMVE and three rolled samples from casting 3K32-A6-VMVF were also characterized. Multiple sections were cut from the original hot-rolled castings. Various orientations from the given cross sections were examined.

In general, the grain sizes measured were in the 25–30 μm range. A few samples had grain sizes on the lower end, 10–20 μm and two samples had larger grain sizes, 25–50 μm . The area fraction of carbide content varied by sample and by casting. ImageJ was used to determine the carbide volume fractions. Rolled plates originating from casting 3K32-A5-VMVE contained carbides ranging between 0.56% and 1.51 vol%. Rolled plate samples from casting 3K32-A6-VMVE carbide content varied between 0.92 vol% and 1.53 vol% and rolled plate samples from casting 3K32-A6-VMVF carbide content varied between 1.12 vol% and 1.20 vol%.

Most samples contained two distinct regions; one region contained equiaxed grains with Mo-rich and Mo-lean areas. It is suspected that this region was from the interior of the original casting. The other distinct region contained an oxygen-rich, feather-like phase. This region appears to have initiated at an edge and seemed to have been squeezed toward the center of the casting, suggesting that it is possibly deformed during the rolling process. These samples also had oxygen-rich phases that appeared to have a flake-like morphology.

One rolled plate sample from casting 3K32-A6-VMVF showed a unique flow pattern in the cross section. The grains followed a distinct hour-glass shape. This appearance could not be explained based on the limited information available on the hot rolled or casting history.

Two hot-rolled plate samples from casting 3K32-A5-VMVE contained large regions of a worm-like inclusion. Based on chemical analysis, this structure appears to be a UO_2 phase. The area fraction of the phase was large, nearly 30%. It is assumed that these were isolated inclusions, but their presence in such large fraction raises concern about whether they exist in other unexamined regions of the rolled plates.

Acknowledgments

This work was funded by the U.S. Department of Energy and the National Nuclear Security Administration under the Material Management and Minimization Reactor Conversion Program and performed at Pacific Northwest National Laboratory (PNNL) under contract DE-AC05-76RL01830. The authors would like to recognize the technical support in material handling and sample preparation by Crystal Rutherford and Anthony Guzman. In addition the authors acknowledge Alan Schemer-Kohn and Nicole Overman for their expertise in electron microscopy and elemental spectroscopy analysis and Luke Sweet for the X-ray diffraction analysis. As indicated in the report, the experimental casting work was performed at the Y-12 Security Complex and shipped to PNNL for characterization.

Contents

Executive Summary	iii
Acknowledgments.....	v
Acronyms and Abbreviations	xi
1.0 Introduction	1.1
2.0 Experimental.....	2.1
2.1 Materials.....	2.1
2.2 Scanning Electron, Optical Light Microscopy, and X-Ray Diffraction Analysis.....	2.2
3.0 Results and Discussion	3.4
3.1 Microstructure of Unidirectional Hot-Rolled 3 mm Plate from Casting 3K32-A5-VMVE.....	3.5
3.2 Microstructure of 3.3mm Hot Cross-Rolled Plate from Casting 3K32-A6-VMVE.....	3.12
3.3 Microstructure of 3.3mm Hot Cross-Rolled Plate from Casting 3K32-A6-VMVF.....	3.13
4.0 Conclusions and Recommendations	4.16
4.1 Conclusions	4.16
4.2 Recommendations	4.16
5.0 Potential Impact of Casting Characterization Results	5.17
6.0 References	6.1
Appendix A – Table of Cast/Rolled Samples Received from Y-12	A.1

Figures

3.1.	Typical optical and BSE-SEM micrographs describing the three type of phases observed in the cast and rolled billets, (a) the as-rolled equiaxed grained microstructure containing both rich and lean regions of Mo, (b) Type “b” with the inhomogeneous, non-stoichiometric, oxygen-rich phase, and (c) Type “c” referring to the worm-like, stoichiometric UO ₂ inclusions.	3.5
3.2.	Optical image of the (a) Sample CF-WA6Y shows the typical hot rolled microstructure from all the samples currently examined, with the black, feather-like, non-stoichiometric oxygen-rich phase found in the center of region.....	3.6
3.3.	Optical image of the sample CF-WA70 (a) rolled cross section showing the Type “a” and Type “b” phase regions, (b) higher magnification optical image of the Type “a” Mo-rich/Mo-lean microstructure and (c) the inhomogeneous, Type “b” oxygen-rich phase region.....	3.7
3.4.	BSE-SEM image of sample CF-WA70 (a) 100X magnification showing the elongated grain structure and the distribution of carbides throughout the microstructure and (b) higher magnification at 250X where the Mo-rich/Mo-lean regions are typified by the light and dark regions.....	3.7
3.5.	BSE-SEM image from the Type “b” region of sample CF-WA70 (a) showing the dark feather-like phase rich in oxygen (b) and the same area analyzed by EDS analysis.....	3.8
3.6.	Optical images of the two sections from hot rolled sample CF-WA71 are shown with (a) an uranium oxide inclusion prevalent and another section from the same sample (b) showing the two regions typically observed (Type a and Type b).	3.9
3.7.	(a) (b) Higher magnification BSE-SEM images of sample CF-WA71 (Figure 3.6 a) containing UO ₂ inclusions and (c) showing the XRD analysis to confirm the phases.....	3.10
3.8.	BSE-SEM image of the two sections from hot rolled sample CF-WA72 are shown in (a) and (b) with a higher magnification view of the fractured carbides in the secondary electron mode of SEM seen in (c).....	3.11
3.9.	Two sections from sample EF-WA6R showing both (a) and (c) the Mo-lean/Mo-rich with fractured carbide region and (b) and (d) the oxygen-rich feather-like phase region.....	3.13
3.10.	Section from sample EF-WA6V shows the typical Mo-lean/Mo-rich region with fractured carbides aligned in the rolling direction.....	3.14
3.11.	(a) Optical image of the section from sample EF-WA6V and (b)(c) BSE-SEM image showing the oxygen-rich, feather-like non-stoichiometric phase also aligned in the rolling direction.	3.15
3.12.	Optical image of the section from rolled sample EF-WA6X showing the Mo-lean/Mo-rich region with fractured carbides aligned in an hour-glass pattern.....	3.15

Tables

2.1. Hot-rolled plate and casting identification including casting thickness and heat treatments.	2.1
3.1. Sample identification and data summary for the as-received rolled billet samples from Y-12.....	3.4
3.2. EDS chemical analysis of structures observed in sample CF-WA70.	3.8
3.3. EDS chemical analysis of structures observed in Figure 3.7 from sample CF-WA71	3.11

Acronyms and Abbreviations

BSE	backscatter electron
EDS	energy-dispersive x-ray spectroscopy
FEG	field emission gun
HIP	hot isostatic processing
HPRR	high-performance research reactor
ID	identification
JEOL	
LABE	low angle backscatter electron
LEU	low enriched uranium
Mo	molybdenum
PNNL	Pacific Northwest National Laboratory
SEM	scanning electron microscopy
U-10Mo	uranium alloyed with 10 wt% molybdenum
Y-12	Y-12 National Security Complex

1.0 Introduction

For several years, research to develop alternate fuels for high-performance research reactors (HPRRs) has been under way to replace high enriched uranium fuel with low enriched uranium (LEU) fuel (Burkes et al. 2009; Burkes et al. 2010a; Burkes et al. 2010b; Snelgrove et al. 1997). To achieve similar ^{235}U content with LEU, given the reactor space constraints, a higher bulk density of fuel is needed, which necessitates the use of monolithic metal alloy fuel. To achieve this density, an alloy that offers a good combination of irradiation performance, oxidation resistance, strength, and ductility is required for HPRR applications (Clark et al. 2006; Mcgeary 1955). Various uranium alloys have been evaluated for their favorable mechanical properties and susceptibility to oxidation and corrosion. Uranium alloyed with 10 wt% molybdenum (U-10Mo) shows improvement in these characteristics compared to similar alloys (Burkes et al. 2009; Burkes et al. 2010a; Burkes et al. 2010b; Clark et al. 2006; Dombrowski 2012; Mcgeary 1955). Several efforts are now under way to optimize the U-10Mo processing parameters and Pacific Northwest National Laboratory (PNNL) has supported these activities (Nyberg et al. 2013). This report summarizes a PNNL study of the effect of alternate casting and processing steps at the Y-12 National Security Complex (Y-12) by examining the microstructure of rolled U-10Mo alloy.

The fabrication process began with U-10Mo alloys being vacuum-induction melted, cast into 25 mm thick ingots followed by a series of hot-rolling steps at Y-12. In this study, the casting thickness was held constant and two different rolling paths were used. It was the intention that these rolled castings would be sheared into coupons, hot rolled with zirconium, and cold rolled to a final thickness of 150-500 μm , thereby eliminating the significant scrap generated by the machining of coupons prepared from cast ingots.

Unlike the previous characterization study performed at PNNL, the material provided by Y-12 was hot-rolled after casting (Nyberg et al. 2013). In the current study, samples were produced at Y-12 under various conditions with the objective of increasing material throughput and process efficiency. For example, the casting thickness was increased to 25.4 mm (1.0 in.) thick and subsequently hot rolled under various conditions. The details of the processing steps used at Y-12 are documented elsewhere (A. L. DeMint et al. 2013a–c). Samples from these hot-rolled plates were then delivered to PNNL for characterization. The material samples were examined for uniformity, grain size, and microstructural inhomogeneities, such as inclusions or atypical phases.

2.0 Experimental

2.1 Materials

PNNL has previously characterized the as-cast microstructure of the U-10Mo alloy. Similarly, the current castings also used Mo rod as a feedstock and were also poured at approximately 1400°C with no hold time prior to casting. However, to increase throughput, the castings were made in 25.4 mm (1.0 in.) thick book molds. All castings were furnace-cooled in the mold to 600°C and then air-cooled to room temperature. Subsequent hot rolling of the castings resulted in 13 samples delivered to PNNL with a final thickness of approximately 3.0 mm (0.12–0.13 in.). **Error! Reference source not found.** provides an overview of the sample matrix with identification methodology for the 13 castings, including the Y-12 Sample identification ID Number (i.e., AP3K32-CF-WA6Y), Y-12 Casting Name (i.e., Leviathan), and Y-12 Casting ID Number (i.e., 3K32-A5-VMVE). Similar information is provided in Appendix A that also includes the PNNL metallography number (i.e., DUM116). *Note that future reference to the Y-12 Hot-Rolled Plate Samples will not include the AP3K32- at the beginning of each identification number.* Each hot-rolled plate sample will be referenced by the last six alphanumeric terms of the ID number, e.g., CF-WA6Y. Specific details of the casting process are classified by Y-12 as Official Use Only/Export Controlled Information and are, therefore, not included in this report. Samples were received and cut from the original rolled plates. Specific locations where samples were removed from the castings were unidentified. Figure 2.1 provides representative images of the as-received sample sections.

Table 2.1. Hot-rolled plate and casting identification including casting thickness and heat treatments.

Y-12 Hot-Rolled Plate Sample ID	Y-12 Casting Name/ID	Y-12 Casting and Rolling Conditions
AP3K32-CF-WA6Y	Leviathan 3K32-A5-VMVE	25.4 mm (1.00 in.) thick casting Unidirectional Hot Rolling to 3.1 mm (0.12 in.) thickness
AP3K32-CF-WA70		
AP3K32-CF-WA71		
AP3K32-CF-WA72		
AP3K32-CF-WA73		
AP3K32-CF-WA74		
AP3K32-CF-WA75		
AP3K32-CF-WA76		
AP3K32-EF-WA6R	Medusa II 3K32-A6-VMVE	25.4 mm (1.00 in.) thick casting Cross-Hot Rolling to 3.3 mm (0.13 in.) thickness
AP3K32-EF-WA6T	Pegasus 3K32-A6-VMVF	25.4 mm (1.00 in.) thick casting Cross-Hot Rolling to 3.3 mm (0.13 in.) thickness
AP3K32-EF-WA6V		
AP3K32-EF-WA6W		
AP3K32-EF-WA6X		



(a)



(b)

Figure 2.1. As-received U-10Mo casting samples from Y-12: (a) CF-WA6Y and (b) EF-WA6W.

2.2 Scanning Electron, Optical Light Microscopy, and X-Ray Diffraction Analysis

For the cross-sectional analysis, the cut sections were cold mounted in an epoxy resin. The mounted samples were successively polished with 600-grit SiC polishing papers down to 6 μm and 1 μm diamond slurries, followed by a final colloidal silica polish. Optical light microscopic images were obtained using an Olympus BX61 optical microscope equipped with polarization filters. Digital images were captured using an Olympus UC50 camera and acquired using PAX-It digital imaging software. The microscope was equipped with objective lenses that could image the sample from 25 to 500X. The grain sizes were measured by standard lineal analysis technique on 100X images. After optical examination, the samples were gold coated for scanning electron microscopy (SEM) analysis. Second-phase particle examination and chemical composition analysis were performed using a JEOL 7600F Field Emission Gun (FEG)-SEM equipped with an Oxford Instruments X-Max 80 mm^2 SDD energy-dispersive x-ray spectroscopy (EDS). Semi-quantitative EDS analysis was performed to determine the variation in chemistry across the microstructure. EDS maps were then generated for a selected microstructure. Electron images were

obtained using a proprietary JEOL low-angle backscatter electron (LABE) detector, an in-lens secondary detector, and a traditional Everhart-Thornley secondary electron detector. The Oxford AZtec software system was used for all EDS analytical analysis.

Quantitative image analysis of carbide and oxygen-rich inclusions were conducted from the backscatter electron (BSE)-SEM images at 100X and 500X magnification and analyzed using ImageJ software. By adjusting the gray color scale, the threshold of the area of interest for both the darker carbides and the lighter oxides could be distinguished separately. The variations in gray color scale and contrast were then quantified and processed using the automated analysis tool. It should be noted that the carbide area fraction was measured in the BSE-SEM mode at low magnification and some variation in these data may be due to slight adjustment to the lighting threshold (brightness, gray-scale, and contrast). This qualitative adjustment can result in variation that will slightly enhance or obscure surface asperities, or artifacts, and thus may have contributed to the differences observed in the resulting values. An example of the threshold adjustment and area quantification is shown in Figure 2.2.

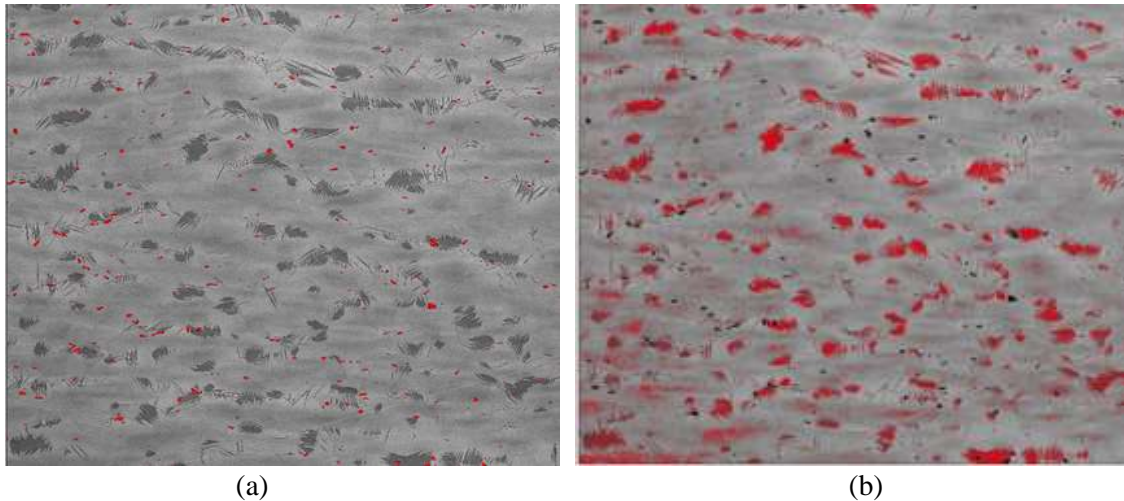


Figure 2.2. Typical micrographs demonstrating the ImageJ threshold analysis to determine microstructural features (in red) such as (a) the area fraction of carbides or (b) the fraction of oxygen-rich phases present within a given view.

X-ray diffraction (XRD) analysis was conducted in a Rigaku Ultima IV equipped with a monochromated Cu K- α X-ray source and a linear position sensitive, silicon strip detector. In general, diffraction data were collected between 25–120° 2 θ in 0.001° increments at a scan rate of 0.5°/min. Full pattern Rietveld refinement was performed using the TOPAS (v4.2) software package from Bruker AXS. Instrument peak shape functions and the instrument zero error were derived from the diffraction profile of National Institute of Standards and Technology-certified reference material 640d (silicon powder). A second order Chebychev Polynomial was used to model the background. Profile convolution functions corresponding to microstructure properties (such as crystallite size and strain) were refined to discriminate between different phases.

3.0 Results and Discussion

The samples received from Y-12 and the corresponding analytical data obtained are identified in

Table 3.1. The microstructural characteristics have been defined as Type a, b, or c and are summarized under a column in Table 3.1 (Composite Microstructure). Composite microstructure was selected because of the number of type of structures observed. Note that Type “a” refers to the standard type of as-rolled microstructure observed, containing both rich and lean regions of Mo. Type “b” refers to rolled samples that contained the inhomogeneous, non-stoichiometric, oxygen-rich phase. Type “c” refers to rolled samples in which the worm-like, stoichiometric UO₂ inclusions were observed. Examples of each of these phases are shown in **Error! Reference source not found.**

Table 3.1. Sample identification and data summary for the as-received rolled billet samples from Y-12.

Y-12 Sample ID	Composite Microstructure	Grain Size (μm)	Area Percent of Carbides (%)	Area Percent of Non-Stoichiometric Oxygen-Rich Phase (%)	Area Percent of UO ₂ (%)
CF-WA6Y	a,b	25-50	1.5	1.1	Not Observed
	a,b	25-50	1.5	1.2	Not Observed
CF-WA70	a,b	10-25	0.8	2	Not Observed
	a,b	10-25	0.8	Unable to Threshold ^(a)	Not Observed
CF-WA71	a,b	10-20	0.6	5.9	Not Observed
	a,c	10-20	Unable to Threshold ^(a)	Not Observed	29.4
CF-WA72	a	25-30	0.8	Not Observed	Not Observed
	a	25-30	0.7	Not Observed	Not Observed
CF-WA73	a	25-30	0.9	Not Observed	Not Observed
	a,b	25-30	0.6	1.5	Not Observed
CF-WA74	a,b	25-30	0.7	1.3	Not Observed
	a,b,c	25-30	Unable to Threshold ^(a)	4.3	Unable to threshold ^(a)
CF-WA75	a,b	25-30	0.9	Unable to Threshold ^(a)	Not Observed
	a,b	25-30	0.9		Not Observed
CF-WA76	a	25-30	0.8	Not Observed	Not Observed
	a	25-30	0.8	Not Observed	Not Observed
EF-WA6R	a	25-30	0.9	Not Observed	Not Observed
	a,b	25-30	1.5	3.1	Not Observed
EF-WA6T	a	25-30	1.0	Not Observed	Not Observed
	a,b	25-30	Unable to Threshold ^(a)		Not Observed
EF-WA6V	a	25-30	1.2	Not Observed	Not Observed
	a,b	25-30	Unable to Threshold ⁽¹⁾		Not Observed
EF-WA6W	a,b	15-20	1.2	1.9	Not Observed
	a,b	15-20	Unable to Threshold ^(a)	5.2	Not Observed
EF-WA6X	a	Up to 50	1.2	Not Observed	Not Observed
	a	15-20	1.2	Not Observed	Not Observed
	a	Up to 50	1.2	Not Observed	Not Observed

(a) Unable to threshold: The different phases obscured each other making the analysis using ImageJ

difficult.

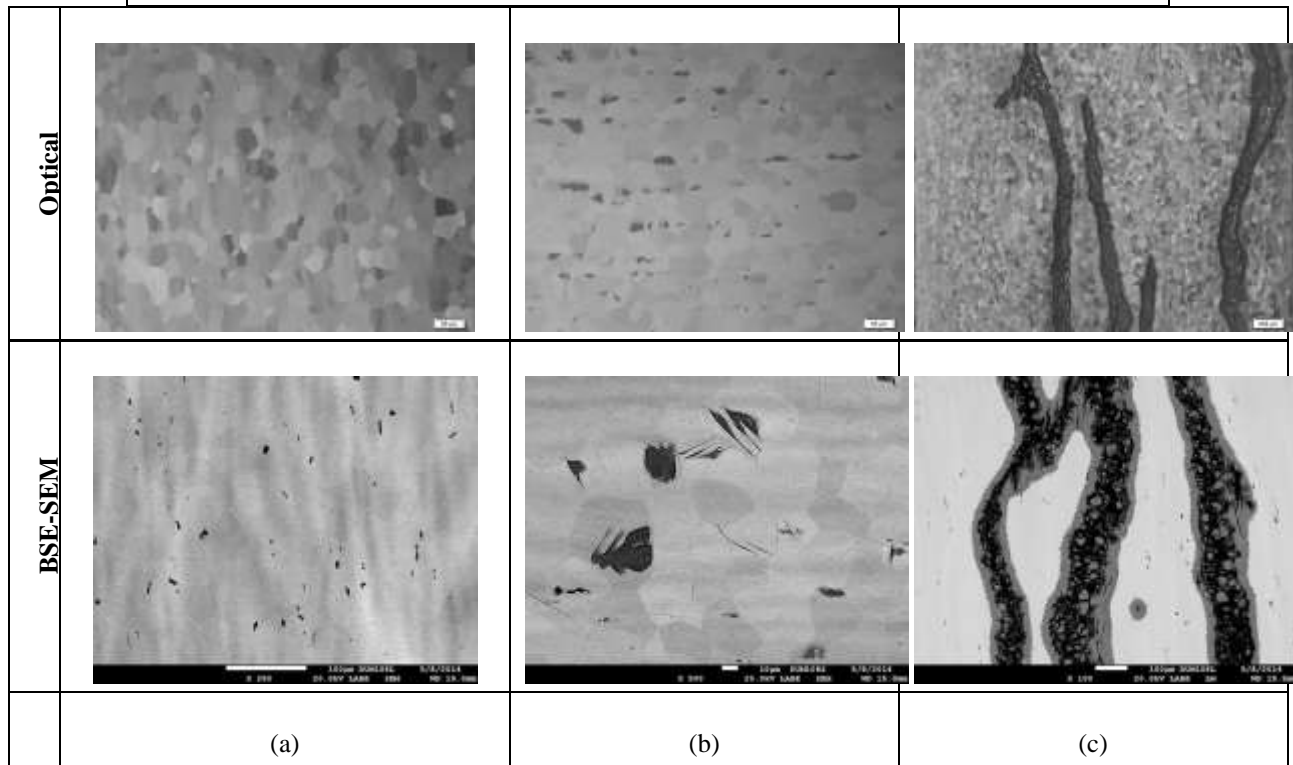


Figure 3.1. Typical optical and BSE-SEM micrographs showing the three type of phases observed in the cast and rolled billets. (a) The as-rolled equiaxed grained microstructure containing both rich and lean regions of Mo, (b) Type “b” with the inhomogeneous, non-stoichiometric, oxygen-rich phase, and (c) Type “c” referring to the worm-like, stoichiometric UO_2 inclusions.

The following sections describe the microstructure of all the samples analyzed in greater detail.

3.1 Microstructure of Unidirectional Hot-Rolled 3 mm Plate from Casting 3K32-A5-VMVE

The microstructure was characterized for eight rolled samples from the casting 3K32-A5-VMVE, rolled to an average thickness 3.1 mm (0.12 in.). In most cases, at least two cross sections were mounted and examined from each sample set. Representative metallographic images and supporting data are shown below.

The typical microstructures observed in sample CF-WA6Y are shown in **Error! Reference source not found.** The rolling direction appears to be in the left-right, horizontal direction. The outside, darker areas in Figure 3.2(a) are the inhomogeneous microstructure containing both Mo-lean and Mo-rich regions. The lighter region in the center of **Error! Reference source not found.**(a) is the non-stoichiometric oxygen-rich phase region and is also shown in **Error! Reference source not found.**(b) and (c). Many of the carbides present appear to be fractured, indicating low temperature or cold rolling was used at some point in the reduction process. Both of the sections from this sample had a microstructure that consisted of two distinct phase regions. The grains were predominately equiaxed, ranging from 25–50 μm in size.

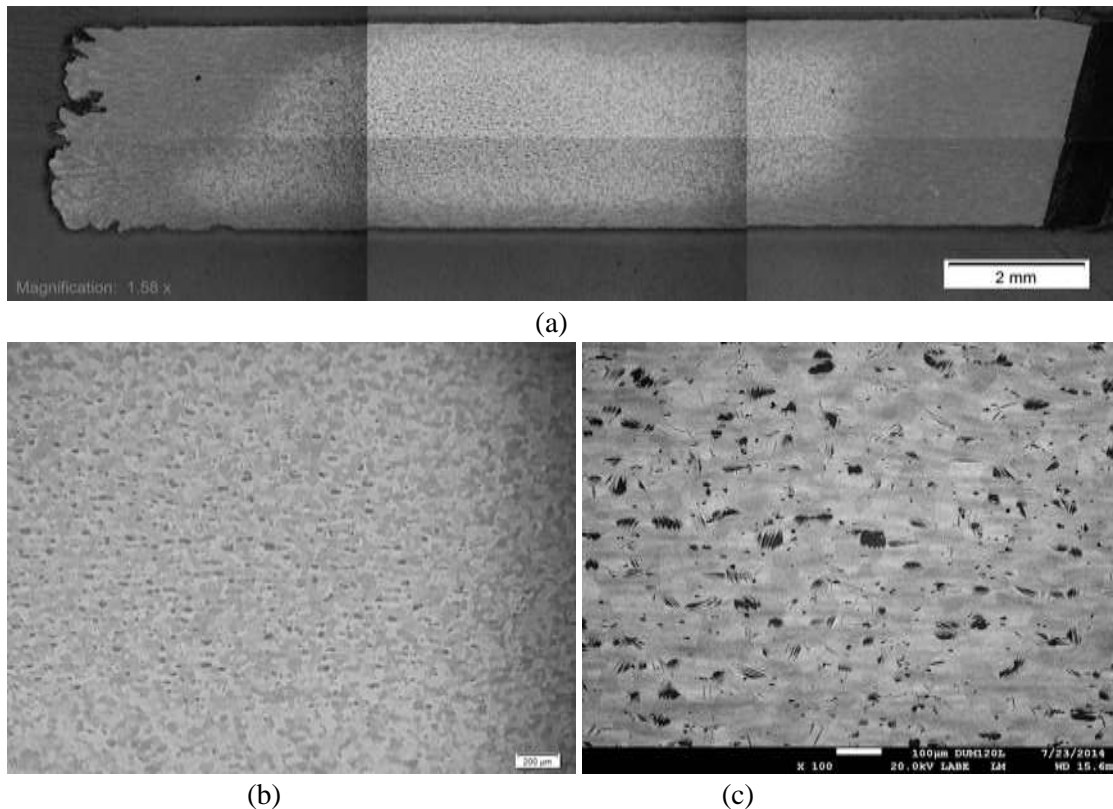
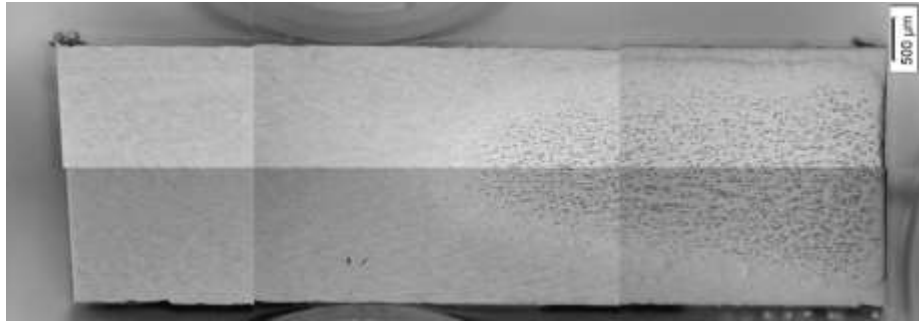


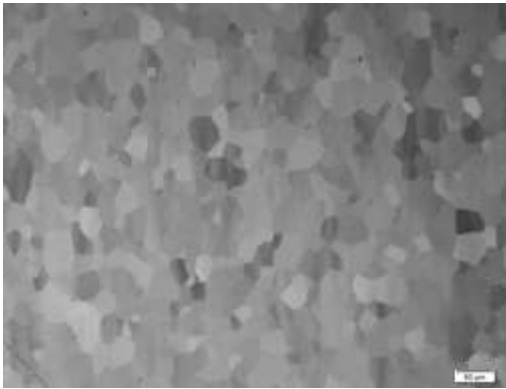
Figure 3.2. Optical image of the (a) Sample CF-WA6Y shows the typical hot-rolled microstructure from all of the samples currently examined, with the black, feather-like, non-stoichiometric oxygen-rich phase found in the center of region. This oxygen-rich phase is shown as observed both (b) optically and (c) using BSE-SEM.

A section from hot-rolled plate sample CF-WA70, originating from casting 3K32-A5-VMVE, is shown in **Error! Reference source not found.** **Error! Reference source not found.**(a) shows the two regions typically observed in most of the hot-rolled plate samples. The Type “a” phase region on the left side contains the Mo-lean/Mo-rich grain structure, and the Type “b” oxide-rich phase region on the right appears to protrude inward from the side of the casting toward the center. It is not known for certain whether the rolling direction was left-to-right or into the plane of the image as shown. In **Error! Reference source not found.**, the Type “a” region is shown in detail and in **Error! Reference source not found.**(c) the two-phase region, Type “b” is shown.

Looking closer at the Type “a”, Mo-rich/Mo-lean, region from sample CF-WA70 using BSE-SEM, one can see further evidence that the carbides have been broken and dispersed as a result of the roll processing and that they primarily appear in the Mo-lean region (**Error! Reference source not found.**). The grain size in this sample averaged between 10–20 μm. In the Type “b”, oxide-rich phase region, further low-angle backscattered images were taken. The dark feather-like structures seen in **Error! Reference source not found.**(b) were confirmed by EDS analysis to be rich in oxygen and uranium. Typical compositional results from the areas identified in **Error! Reference source not found.**(b) are listed in Table 3.2.



(a)

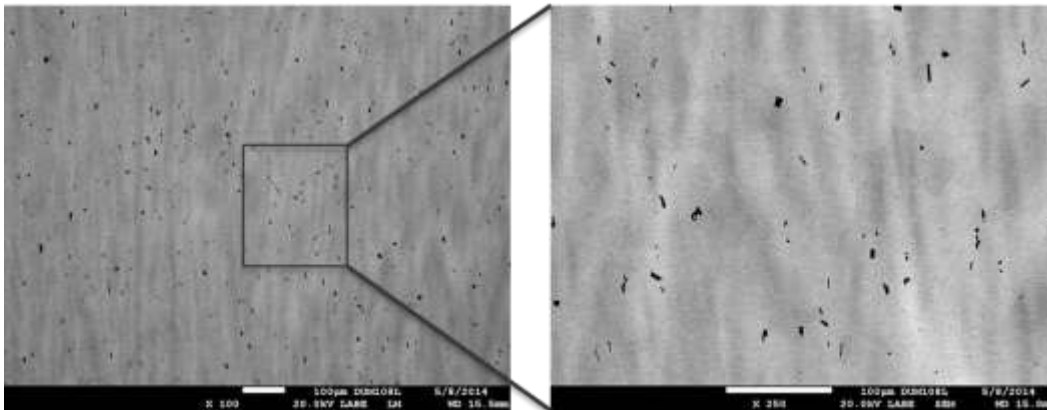


(b)



(c)

Figure 3.3. Optical image of the sample CF-WA70 (a) rolled cross section showing the Type “a” and Type “b” phase regions, (b) higher magnification optical image of the Type “a” Mo-rich/Mo-lean microstructure, and (c) the inhomogeneous, Type “b” oxygen-rich phase region.



(a)

(b)

Figure 3.4. BSE-SEM image of sample CF-WA70 (a) 100X magnification showing the elongated grain structure and the distribution of carbides throughout the microstructure, and (b) higher magnification at 250X where the Mo-rich/Mo-lean regions are typified by the dark and light regions respectively.

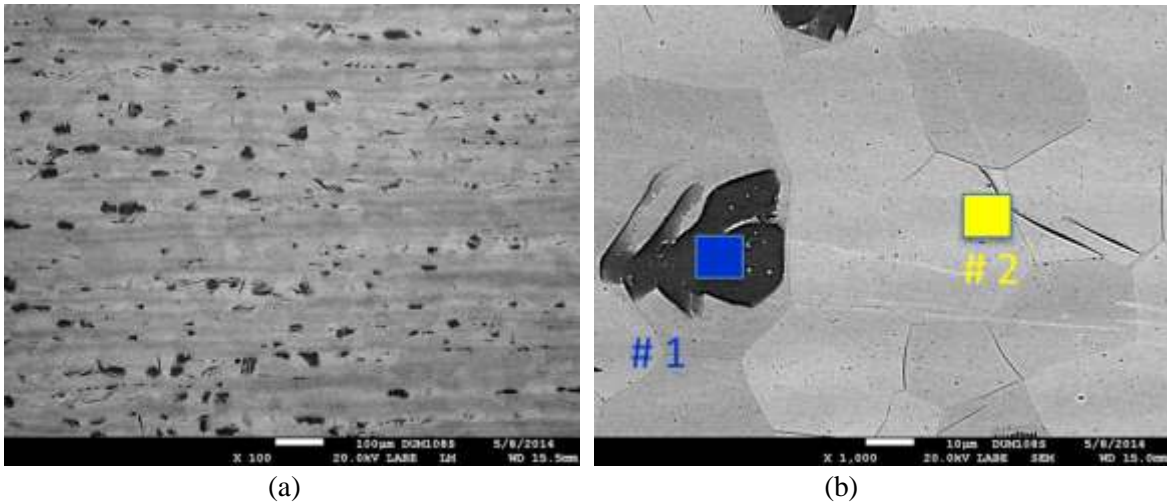
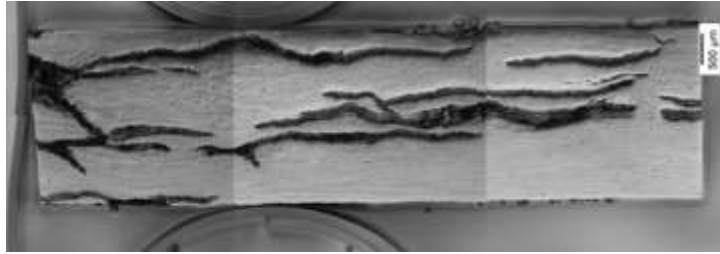


Figure 3.5. BSE-SEM image from the Type “b” region of sample CF-WA70 (a) showing the dark feather-like phase rich in oxygen (b) and the same area analyzed by EDS analysis.

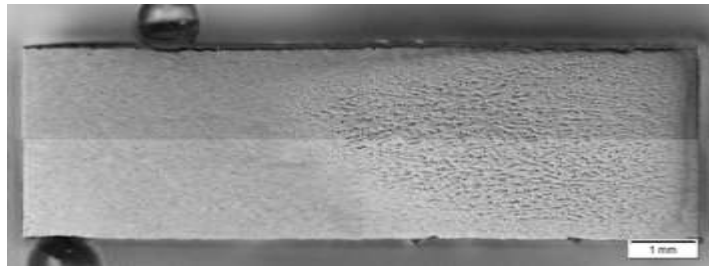
Table 3.2. EDS chemical analysis of structures observed in sample CF-WA70.

Spectrum Label	Weight %				
	O	Si	Mo	U	Total
#1	3.22	0.11	8.82	87.86	100.00
#2	1.86	0.12	10.26	87.77	100.00

Next, two sections from hot-rolled sample CF-WA71 were examined and are shown in **Error! Reference source not found.** This sample contained an inclusion that had a worm-like appearance that stretched across the entire cross section of section A, as shown in **Error! Reference source not found.**(a). The second section examined from this same sample did not contain such an inclusion and appeared much like the other samples with two distinct regions of the casting. A closer examination of the inclusion, shown in **Error! Reference source not found.**, revealed multiple features, an outer reaction zone surrounding an inner region of dispersed oxide-rich particles of uranium. The composition of the inclusion, listed in Table 3.3, is confirmed by EDS and XRD (Figure 3.7c) to contain UO_2 . It is not known whether this inhomogeneity was from the skull, which may have been entrained during the casting process, or from another source. In addition the Na, Si, and Ni may have been entrained in the open pores during rolling, cutting, or sample preparation. Sources of those elements will require more detailed study of the Y12 and PNNL process materials and were not determined during this work. In general, this sample had a microstructure similar to the WA-70 sample, with a composite microstructure of oxygen-rich phases and a fine-grained microstructure. The microstructure consisted of two distinct phases and contained equiaxed grains 10–20 μm in diameter. As with the other sections from the same sample, it appears to be a rolled microstructure.



(a)



(b)

Figure 3.6. Optical images of the two sections from hot-rolled sample CF-WA71 are shown with (a) Type “c” microstructure; the worm-like, stoichiometric UO_2 inclusions, and (b) showing the composite of Type a and Type b the as-rolled equiaxed grained microstructure containing both rich and lean regions of Mo, and with the inhomogeneous, non-stoichiometric, oxygen-rich phase respectively.

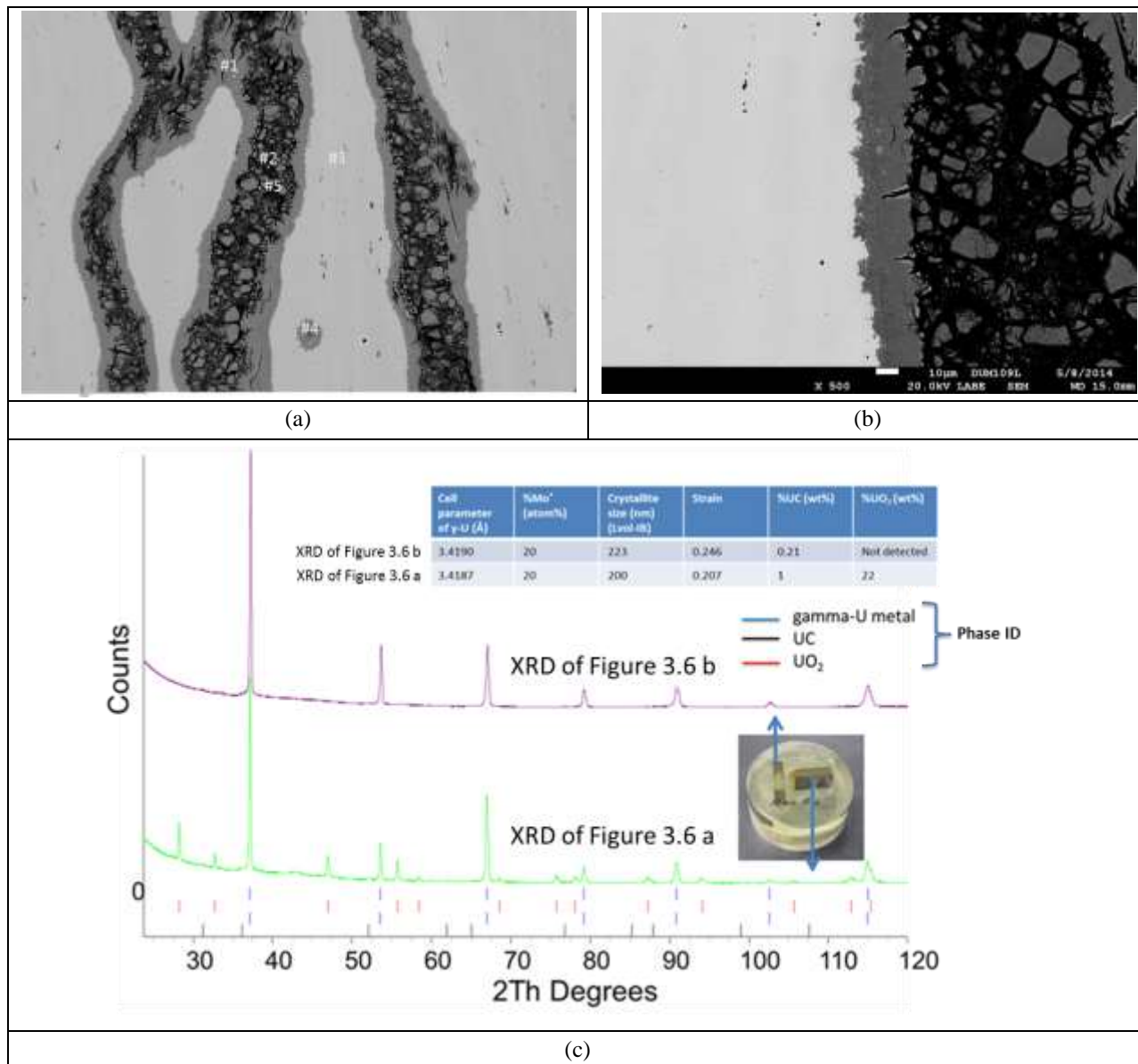


Figure 3.7. (a) (b) Higher magnification BSE-SEM images of sample CF-WA71 (**Error! Reference source not found.**a) containing UO₂ inclusions and (c) showing the XRD analysis to confirm the phases.

Table 3.3. EDS chemical analysis of structures observed in Figure 3.7 from sample CF-WA71

Spectrum Label	Weight %				
	#1	#2	#3	#4	#5
O	13.25	13.37	4.76	10.54	12.51
Na	-	1.21	-	-	-
Si	-	0.59	-	-	-
Ni	-	0.61	-	-	-
Mo	3.07	1.41	8.54	6.51	-
U	83.68	82.81	86.69	82.95	86.67
Total	100.0	100.0	100.0	100.0	100.0

Next, two sections were examined from rolled sample CF-WA72, that originated from casting 3K32-A5-VMVE. The typical Mo-lean/Mo-rich region was observed in both sections and is shown in **Error! Reference source not found.** The nominal grain size was 25–30 μm . No dual phase or oxygen-rich phase was observed. The carbides in both sections were clearly visible, appear to have been broken down during the rolling process, and primarily appear in the Mo-lean region(**Error! Reference source not found.**(c)). The amount of carbide present was measured to be about 0.7% as measured by area percent.

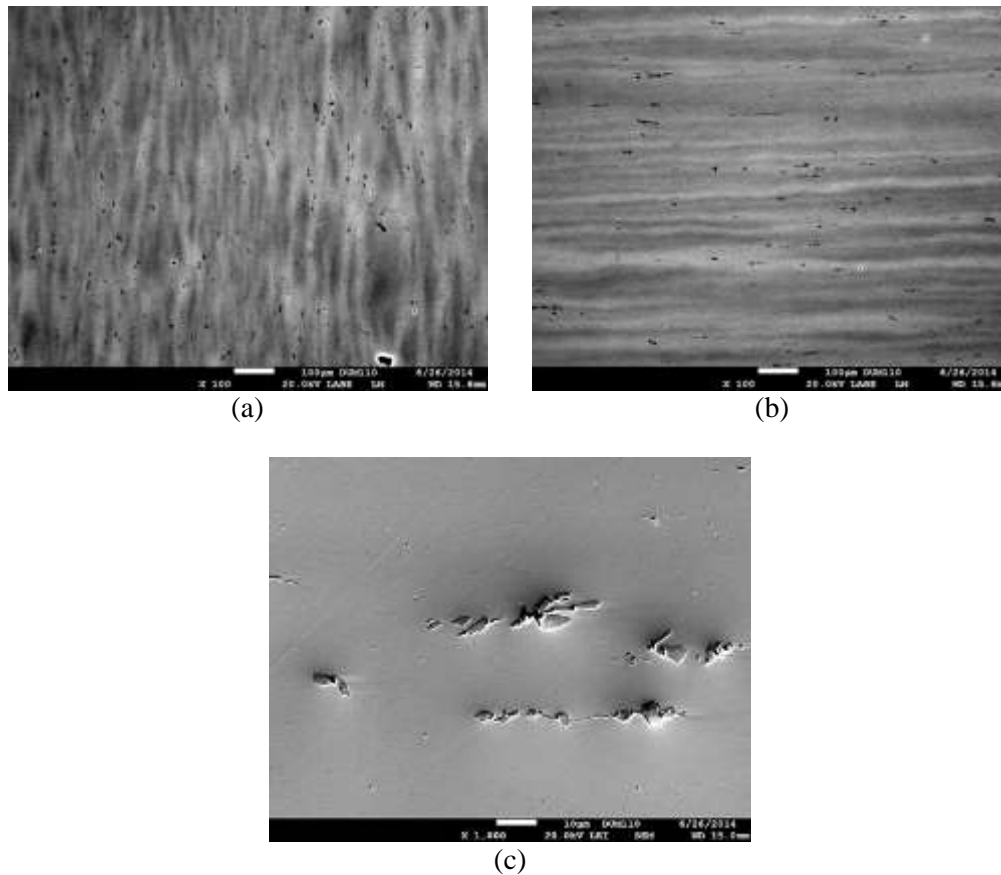


Figure 3.8. BSE-SEM image of the two sections from hot-rolled sample CF-WA72 are shown in (a) and (b) with a higher magnification view of the fractured carbides in the secondary electron mode of SEM seen in (c).

Sections from hot-rolled samples CF-WA73 through CF-WA76, also from casting 3K32-A5-VMVE, all exhibited microstructures similar to those previously described, namely having a Type “a,” Mo-lean/Mo-rich region and a Type “b” region, with the oxygen-rich, non-stoichiometric phase as previously observed. Sample CF-WA74 also contained the third type of phase, the worm-like, oxygen-rich inclusions.

3.2 Microstructure of 3.3mm Hot Cross-Rolled Plate from Casting 3K32-A6-VMVE

The microstructure was characterized for the two rolled samples received from the second casting 3K32-A6-VMVF (average thickness 0.13 in.). As before, cross sections were mounted and examined from each sample set. Images and/or description are given below for each sample.

In **Error! Reference source not found.**, micrographs from rolled sample EF-WA6R are shown. **Error! Reference source not found.**(a) and 3.9(b) are low magnification optical images from two separate sections of the same sample. **Error! Reference source not found.**(c) is a BSE-SEM image from the section shown in **Error! Reference source not found.**(a), and **Error! Reference source not found.**(d) is an BSE-SEM image from the section shown in Figure 3.9(b). Similar to the microstructure observed in the previous sample, areas with two distinct phases were present, namely a region with a Mo-lean/Mo-rich segregated region containing fractured carbides along the rolling direction (**Error! Reference source not found.**(a) and 3.9(c)), and areas containing the oxygen-rich, non-stoichiometric phase within the grains having a feather-like appearance (**Error! Reference source not found.**(b) and (d)). Average grain size is 25–30 μm and again it appears to be a rolled microstructure containing between 0.92 and 1.53 area fraction carbides.

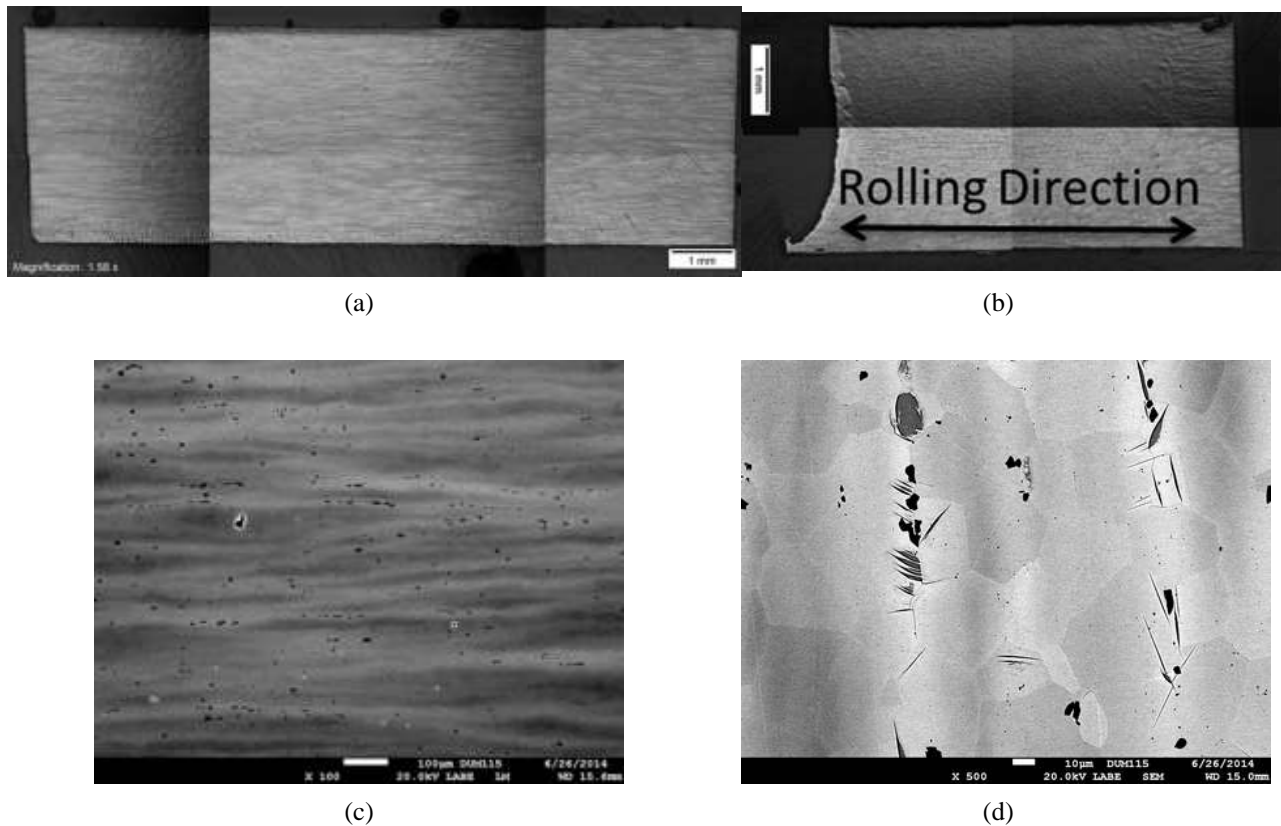


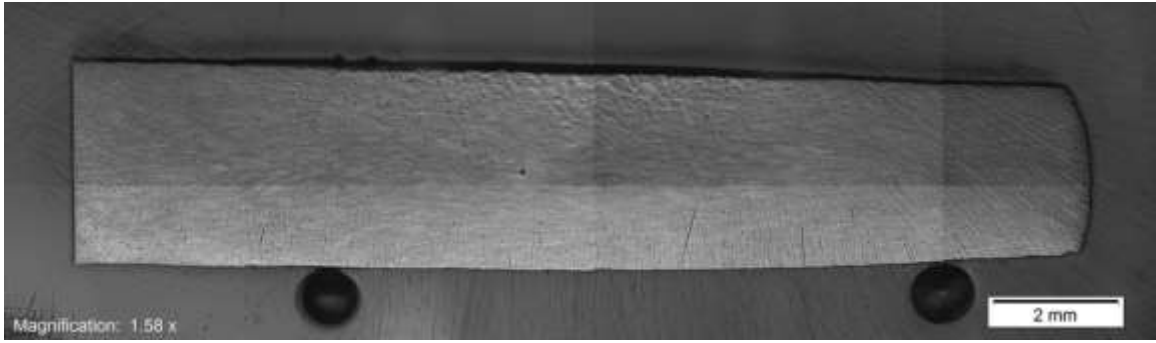
Figure 3.9. Two sections from sample EF-WA6R showing both (a) and (c) the Mo-lean/Mo-rich with fractured carbide region and (b) and (d) the oxygen-rich feather-like phase region.

The microstructure observed in rolled sample EF-WA6T was essentially identical to that observed in EF-WA6R. The area percent of carbide was measured as 0.95% and was also quite similar to the other rolled sample from casting 3K32-A6-VMVE.

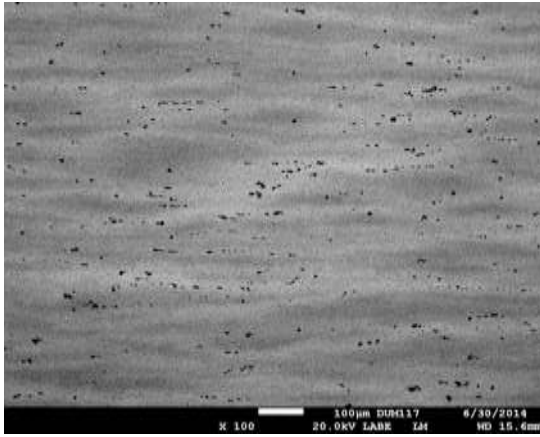
3.3 Microstructure of 3.3mm Hot Cross-Rolled Plate from Casting 3K32-A6-VMVF

The microstructures for the final three rolled samples (EF-WA6V, EF-WA6W, and EF-WA6X) from casting 3K32-A6-VMVF (average thickness 0.13 in.) were examined. Again, consistent with the other rolled castings, the same type of microstructural features and phases were observed. Typical images are provided in the micrographs shown in **Error! Reference source not found.** The Mo-lean/Mo-rich structure is shown in detail in **Error! Reference source not found.** and the oxygen-rich, feather-like appearing non-stoichiometric phase is shown in **Error! Reference source not found.**

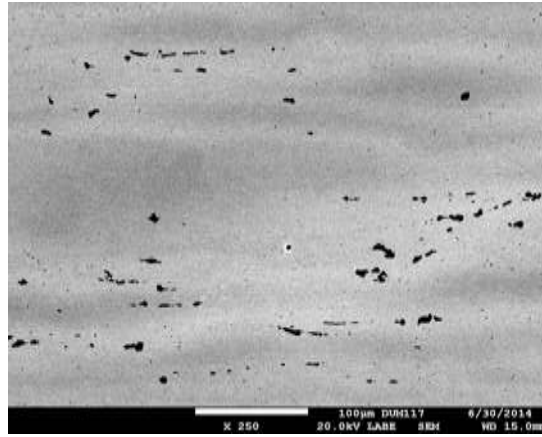
The one notable difference observed in this rolled section was that the material flow in one sample (EF-WA6W) was not linear. This was evident by the curved, hour-glass flow pattern of the grains shown in **Error! Reference source not found.** It is not understood what caused such unusual material flow under normal rolling conditions. The micrographs and description for these samples are shown below.



(a)



(b)



(c)

Figure 3.10. Section from sample EF-WA6V shows the typical Mo-lean/Mo-rich region with fractured carbides aligned in the rolling direction. (a) Optical image (b) and (c) BSE-SEM image.

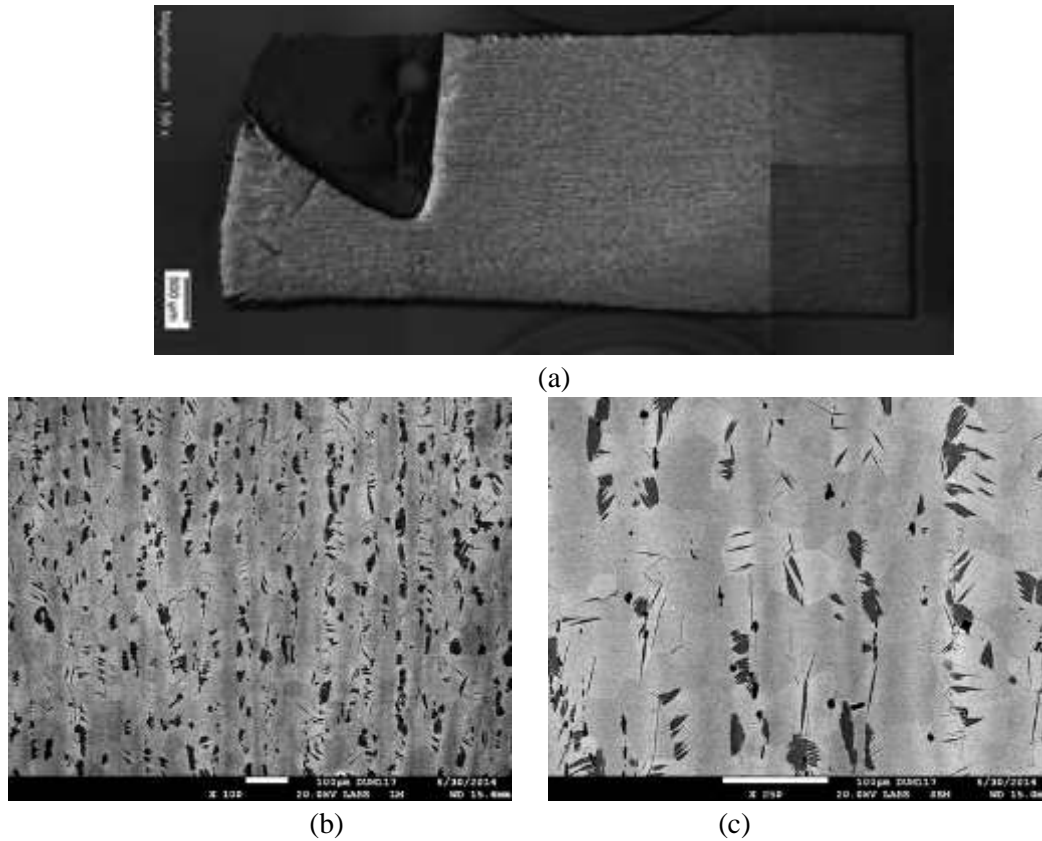


Figure 3.11. (a) Optical image of the section from sample EF-WA6V and (b)(c) BSE-SEM image showing the oxygen-rich, feather-like non-stoichiometric phase also aligned in the rolling direction.

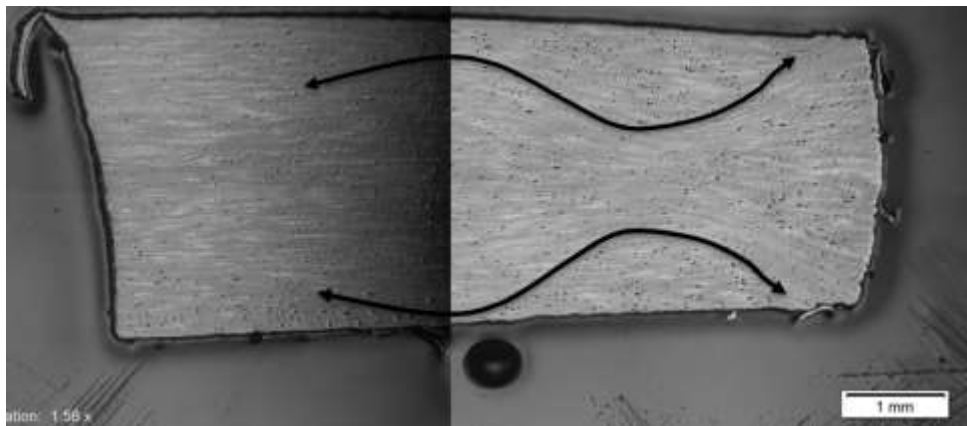


Figure 3.12. Optical image of the section from rolled sample EF-WA6X showing the Mo-lean/Mo-rich region with fractured carbides aligned in an hour-glass pattern.

4.0 Conclusions and Recommendations

A characterization study was conducted at PNNL on hot-rolled U-10Mo cast billets produced at Y-12. This study has been useful in evaluating how the casting process for 25.4 mm (1.0 in.) thick castings with subsequent hot rolling produced a variety of microstructural features. This work might help to identify unintended changes in microstructure and composition if such a casting process is used. Based on the specific castings evaluated, the following conclusions and recommendations are provided.

4.1 Conclusions

1. Typically the microstructure observed from the samples taken from the various rolled plates that originated from three separate castings in this study had two distinct phases:
 - A region with equiaxed grains ranging in size between 10–50 μm , with the average being in the range of 25–30 μm
 - Elongated, feather-like phase rich in oxygen, and non-stoichiometric.
2. There was inhomogeneity across the microstructure, with Mo-lean and Mo-rich regions.
3. Overall, it appears to be a rolled microstructure, with fine carbides broken along the rolling direction.
4. Typical carbide content observed was approximately 1% +/- 0.3% areal percent.
5. No gross porosity was observed.
6. No coarse carbides (i.e., greater than 20 μm) were observed.
7. Hot-rolled plates originating from thicker castings, such as those used in this study, appear to be a viable option for improved efficiency, but further process optimization is required.

4.2 Recommendations

While anomalous structures were observed in the rolled plates, it appears that the thick casting/hot-rolling processing route may produce very high-quality materials. The billets obviously need to be homogenized to eliminate/minimize Mo segregation and prevent the banded microstructure. However, when the microstructure is examined away from the anomalous phases and the Mo banding is ignored, the material is sound; it possesses equiaxed grains and minimal porosity associated with the carbide fracture. A good example is the optical metallography of Figure 3.1a where Mo banding cannot be seen by optical microscopy and the U-10Mo is a very consistent equiaxed grain sized material. Given that the process looks viable, the following recommendations can be made:

- The billet must be homogenized to eliminate Mo segregation; given the thickness of the billet and the reduced solidification and cooling rates it would be expected that the homogenization conditions would be different than those recommended by PNNL for the 5 mm castings (Joshi et al 2013). A homogenization study is needed.
- The low-density (Z number) inclusions are likely from two sources: 1) the skull or 2) a skin formed during mold fill. This type of casting defect can be addressed through mold and orifice design. The ongoing modeling work at Los Alamos National Laboratory should be able to predict a hot top configuration to capture the skull, and likewise the mold fill modeling should be able to optimize the

orifice and mold configuration to prevent skin entrainment (Dombrowski et al 2014). A model of the billet casting process and mold should be prepared and used to predict a new mold and orifice design.

5.0 Potential Impact of Casting Characterization Results

The current work indicated that the rolled sections originating from the thicker 25.4 mm (1.0 in.) thick U-10Mo castings can exhibit a high-quality uniform structure. Anomalous structures observed may be resolved by homogenization of the casting prior to rolling and a new casting mold design. The thicker casting certainly allows for more options for coupon fabrication and should improve overall process yield.

6.0 References

- Burkes DE, T Hartmann, R Prabhakaran, and J-F Jue. 2009. "Microstructural Characteristics of DU-x Mo Alloys with x = 7 - 12 Wt%." *Journal of Alloys and Compounds* 479(1-2):140-147. doi: <http://dx.doi.org/10.1016/j.jallcom.2008.12.063>.
- Burkes DE, CA Papesch, AP Maddison, T Hartmann, and FJ Rice. 2010a. "Thermo-Physical Properties of DU-10 Wt% Mo Alloys." *Journal of Nuclear Materials* 403(1-3):160-166. doi: <http://dx.doi.org/10.1016/j.jnucmat.2010.06.018>.
- Burkes DE, R Prabhakaran, T Hartmann, J-F Jue, and FJ Rice. 2010b. "Properties of DU-10 Wt% Mo Alloys Subjected to Various Post-Rolling Heat Treatments." *Nuclear Engineering and Design* 240(6):1332-1339. doi: <http://dx.doi.org/10.1016/j.nucengdes.2010.02.008>.
- Clark CR, JF Jue, GA Moore, NP Hallinan, and BH Park. 2006. "Update on Monolithic Fuel Fabrication Methods." *The 2006 RERTR International Meeting*, Cape Town, South Africa, Oct 29. – Nov. 3, 2006.
- DeMint AL, Gooch JG, Crane KR, and Fleury DE. 2013a. "Uranium-10% Molybdenum Billet Rolling Study 1: *Casting*." Y/DV-2311, Y-12 National Security Complex, Oak Ridge, Tennessee 37831.
- DeMint AL, Gooch JG, Crane KR, and Fleury DE. 2013b. "Uranium-10% Molybdenum Billet Rolling Study 2: *Rolling*." Y/DV-2313, Y-12 National Security Complex, Oak Ridge, Tennessee 37831.
- DeMint AL, Gooch JG, Crane KR, and Fleury DE. 2013c. "Uranium-10% Molybdenum Billet Rolling Study 3: *Cutting and Heat Treating*." Y/DV-2314, Y-12 National Security Complex/DIto
- Dombrowski DE. 2012. Overview of LANL Progress in Process Development, Advanced Characterization Methods and Prototype Fabrication. In *Proceedings of RERTR 2012, 34th International Meeting on Reduced Enrichment for Research and Test Reactors*, Warsaw, Poland.
- Dombrowski DE, RM Aikin, KD Clarke, T Lienert, PO Dickerson, and LA Tucker. 2014. LANL Progress on UMo Fuel Fabrication Process Development. In *Proceedings of RERTR 2014, 35th International Meeting on Reduced Enrichment for Research and Test Reactors*, Vienna, Austria, October 12-16, 2014.
- Joshi VV, EA Nyberg, CA Lavender, D Paxton, H Garmestani, and DE Burkes. 2013. "Thermomechanical Process Optimization of U-10wt% Mo – Part 1: High-Temperature Compressive Properties and Microstructure." *Journal of Nuclear Materials* (Available online, published 11/14/13). doi:<http://dx.doi.org/10.1016/j.jnucmat.2013.10.065>.
- Mcgeary RK. 1955. *Development and Properties of Uranium-Base Alloys Resistant to Corrosion in High-Temperature Water*. USAEC Report WAPD-127 Part I, Westinghouse Electric Corporation, Atomic Power Division, Pittsburgh, P.O. Box 1468, Pennsylvania.
- Nyberg EA, Joshi, VV, Lavender CA, Paxton DM, Burkes, DE. 2013. *The Influence of Casting Conditions on the Microstructure of As-Cast U-10Mo Alloys: Characterization of the Casting Process Baseline*. PNNL-23049, Pacific Northwest National Laboratory, Richland, Washington.

Snelgrove JL, GL Hofman, MK Meyer, CL Trybus, and TC Wiencek. 1997. "Development of Very-High-Density Low-Enriched-Uranium Fuels." *Nuclear Engineering and Design* 178(1):119–126. doi: [http://dx.doi.org/10.1016/S0029-5493\(97\)00217-3](http://dx.doi.org/10.1016/S0029-5493(97)00217-3).

Appendix A

Table of Cast/Rolled Samples Received from Y-12

PNNL Met ID	Y-12 Rolled Plate Sample ID	Y-12 Casting Name and ID	Casting Thickness and Rolling Condition
DUMo120	AP3K32-CF-WA6Y	Leviathan 3K32-A5-VMVE	25.4 mm (1.00 in.) thick casting Unidirectional Hot Rolling to 3.1 mm (0.12 in.) thickness
DUMo108	AP3K32-CF-WA70		
DUMo109	AP3K32-CF-WA71		
DUMo110	AP3K32-CF-WA72		
DUMo111	AP3K32-CF-WA73		
DUMo112	AP3K32-CF-WA74		
DUMo113	AP3K32-CF-WA75		
DUMo114	AP3K32-CF-WA76		
DUMo115	AP3K32-EF-WA6R	Medusa II 3K32-A6-VMVE	25.4 mm (1.00 in.) thick casting Cross-Hot Rolling to 3.3 mm (0.13 in.) thickness
DUMo116	AP3K32-EF-WA6T		
DUMo117	AP3K32-EF-WA6V	Pegasus 3K32-A6-VMVF	25.4 mm (1.00 in.) thick casting Cross-Hot Rolling to 3.3 mm (0.13 in.) thickness
DUMo118	AP3K32-EF-WA6W		
DUMo119	AP3K32-EF-WA6X		

Distribution

<u>No. of Copies</u>		<u>No. of Copies</u>	
1	Department of Energy National Nuclear Security Administration Global Threat Reduction Initiative 1000 Independence Ave. Washington, DC 20002 Mr. Christopher Landers Mr. Bryan Reed	5	Local Distribution Pacific Northwest National Laboratory Eric Nyberg K2-03 Vineet Joshi K2-03 Curt Lavender K2-03 Mario Pereira K8-46 Douglas Burkes K8-34
1	Idaho National Laboratory P.O. Box 1625 Idaho Falls, ID 83415 Mr. Kenneth Rosenberg Dr. Barry Rabin		
1	Argonne National Laboratory 9700 S Cass Ave. Argonne, IL 60439 Dr. Erik Wilson		



Pacific Northwest
NATIONAL LABORATORY

*Proudly Operated by **Battelle** Since 1965*

902 Battelle Boulevard
P.O. Box 999
Richland, WA 99352
1-888-375-PNNL (7665)
www.pnnl.gov



U.S. DEPARTMENT OF
ENERGY